4) Estimation of ground motion

Estimation of ground motion generally consists of two processes as shown in Figure 2.3.8-17. The first process represents the estimation of ground motion at bedrock and the second process represents the estimation of local site effects. The ground motion at surface can be estimated when both processes are calculated.

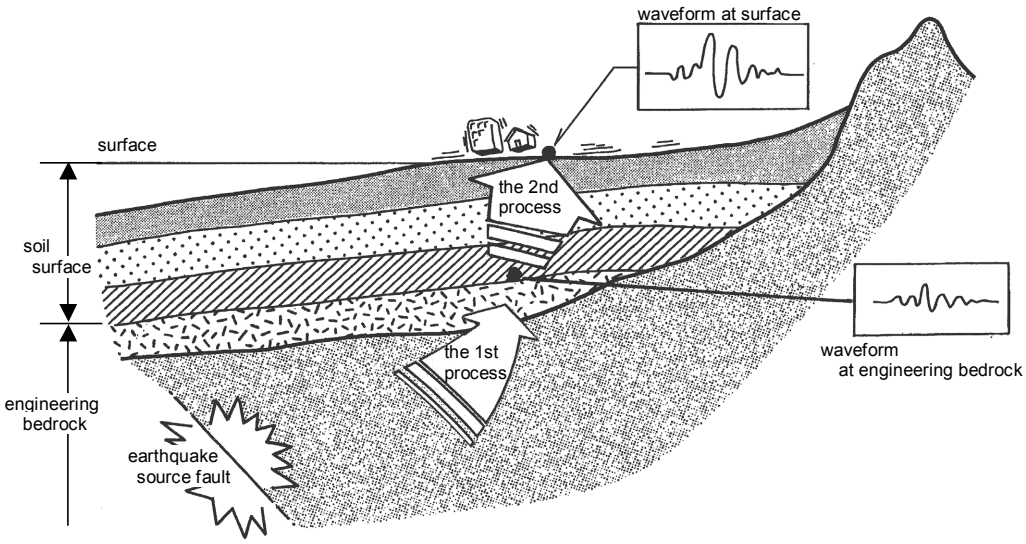

Figure 2.3.8-17 Schematic illustration of wave propagation

The 1st Process: Wave propagation in bedrock

The 2nd Process: Wave propagation in soil surface

a) Estimation of ground motion at bedrock (the 1st process)

Outline of the Method

Waveform at bedrock is calculated using the attenuation formula of response spectrum, empirical envelope function and random phase. The flow chart of this method is shown in Figure 2.3.8-18(Association for the development of earthquake prediction, 1998).

(a) Setting of target response spectrum with 5% damping
(b) Assumption of initial Fourier amplitude spectrum, for which target response spectrum with 5% damping is used
(c) Setting of Fourier phase spectrum with random phase
(d) Carrying out Fourier inverse transform with above Fourier amplitude spectrum and Fourier phase spectrum in order to get waveform in time domain
(e) Multiplying waveform by envelope function in order to get modified waveform in time domain
(f) Calculation of response spectrum with 5% damping from modified waveform
(g) Getting modified Fourier amplitude spectrum by multiplying (amplitude of target

response spectrum)/(calculated response spectrum)

(h) Iteration of process from d) to g) until the difference between target response spectrum and calculated response spectrum become small

(i) The calculated waveform is thus acquired.

We used the attenuation relation of Shumidt et al. (1997) as the target response spectrum, and modified Jennings type function (Hisada et al., 1976) as the envelope function $E(t)$. Random phase ϕ_i is given by random number between 0 and 2π. We assumed that the bedrock corresponds to the stratum with S-wave velocity of more than 750m/s for Guatemala City, Quezaltenango and Escuintla, 650m/s for Mazatenango, and more than 450m/s for Puerto Barrios.

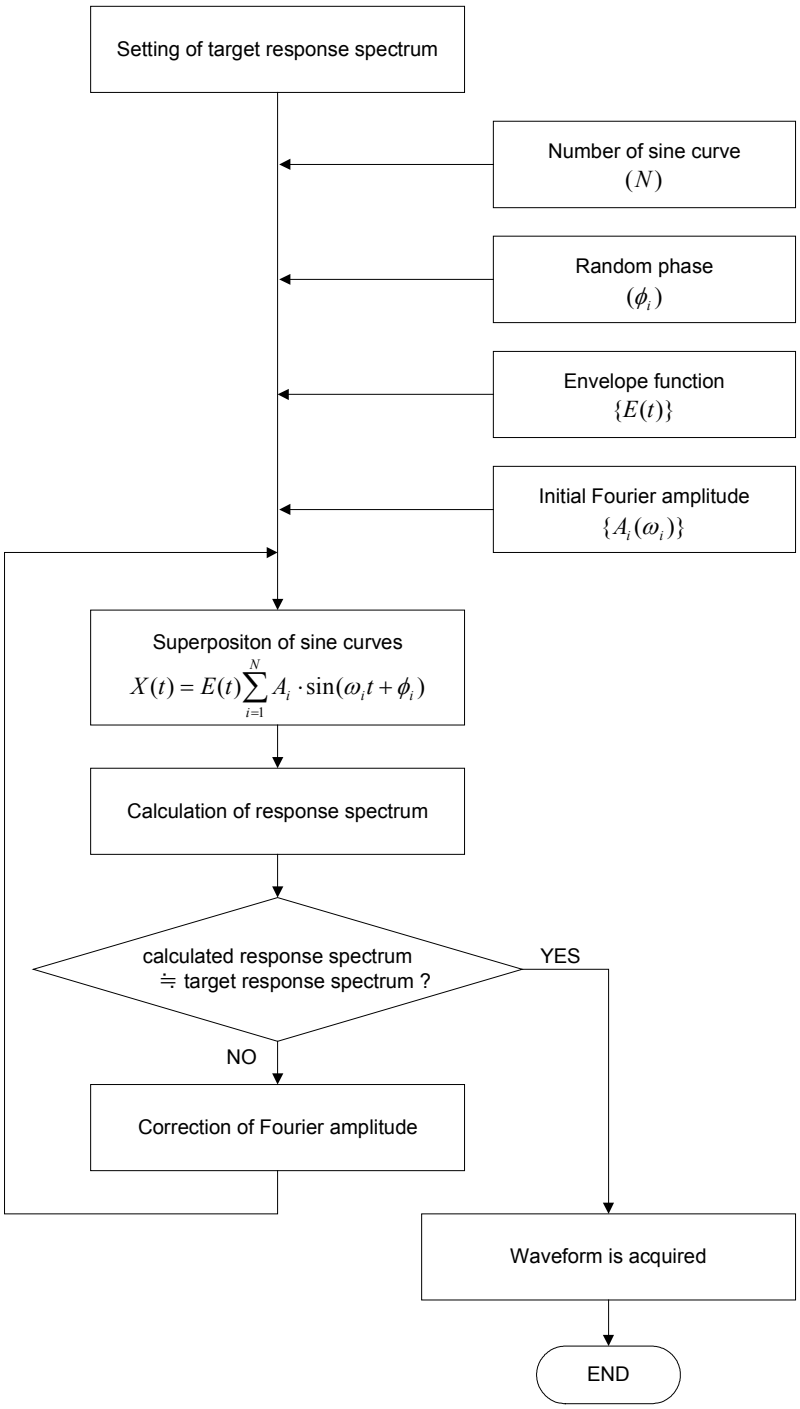

Figure 2.3.8-18 Flow chart of estimation of ground motion at bedrock

b) Estimation of local site effects (the 2nd process): Equivalent linear approach of non-linear response

In general, it is a characteristic of soil that as shear strain increases, shear modulus is reduced and the damping factor is increased. For this method, the calculation is executed with the following steps in order to consider this non-linear behavior of surface soil (see also Figure 2.3.8-19).

Step (1) Modeling of soil structure with parameters necessary for calculation and calculation of shear modulus and damping factor on the assumption of a slight shear strain

Step (2) Execution of multiple reflection analysis for given incident waveform and calculation of time series of shear strain for each layer

Step (3) Calculation of new shear modulus and damping factor corresponding to 60 percent of maximum shear strain, which is given by response analysis, using strain-dependent curves of shear modulus and damping factor

Step (4) Calibration of soil structure model with newly gained shear modulus and damping factor

Step (5) Iteration of the calculation from Step (2) to Step (4) until shear modulus and damping factor converge

In Guatemala, no experimental value has been acquired for strain-dependent curves of shear modulus and damping factor (M. Matus and R. Escobar, personal communication, 2002). Therefore, we used in this analysis the strain-dependent curves of shear modulus and damping factor stipulated as the criteria of the Japanese Government.

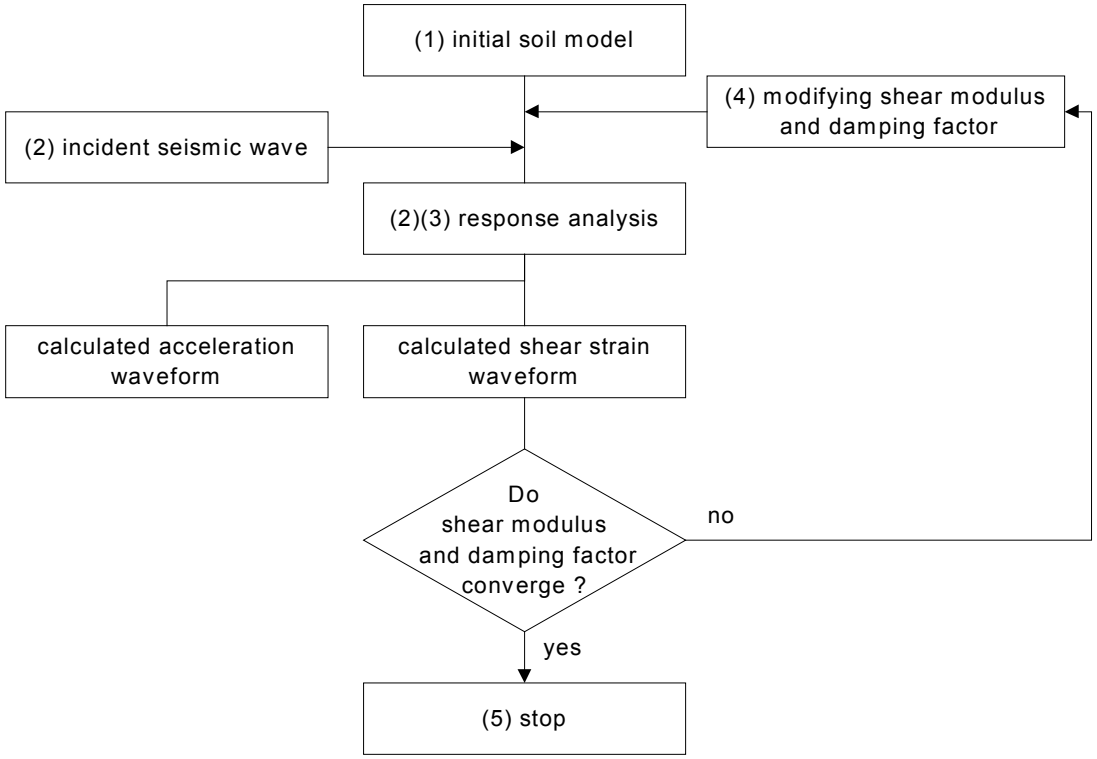

Figure 2.3.8-19 Flow chart of equivalent linear approach

c) Evaluation indexes for ground motion

The estimation results of ground motion are indicated in the modified Mercalli intensity.

The relationship between the modified Mercalli intensity and the ground motion is reported as follows; it has high correlation with the acceleration at the low seismic intensity and has high correlation with the velocity at the high seismic intensity (Wald et al., 1999). Furthermore, the disaster of building and the velocity are deemed well correlated. Therefore, for the calculation of the modified Mercalli intensity, the method of Wald et al. (1999) in which the intensity is calculated from the acceleration for the area with low seismic intensity and from the velocity for the area with high seismic intensity is used.

The record of earthquake observed at the Universidad de San Carlos in Guatemala City at the time of the Guatemala earthquake in 1976 is restored as the seismic waveform by Knudson and Perez. According to this record, the maximum acceleration of the horizontal components of ground motion is approximately 200 cm/s2. The seismic intensity near the Universidad de San Carlos at the time of the Guatemala earthquake reached Level VII. The results of calculation by Wald et al. (1999) are not inconsistent with the maximum acceleration of 200 cm/ s2 and the seismic intensity of Level VII.

5) Estimation of liquefaction potential

The liquefaction potential is estimated in a flow shown in Figure 2.3.8-20. The estimation technique for liquefaction potential, first proposed by Seed (1979), has been improved by several researchers ever since. The technique used in this study was devised by Japan Road Association (1996).

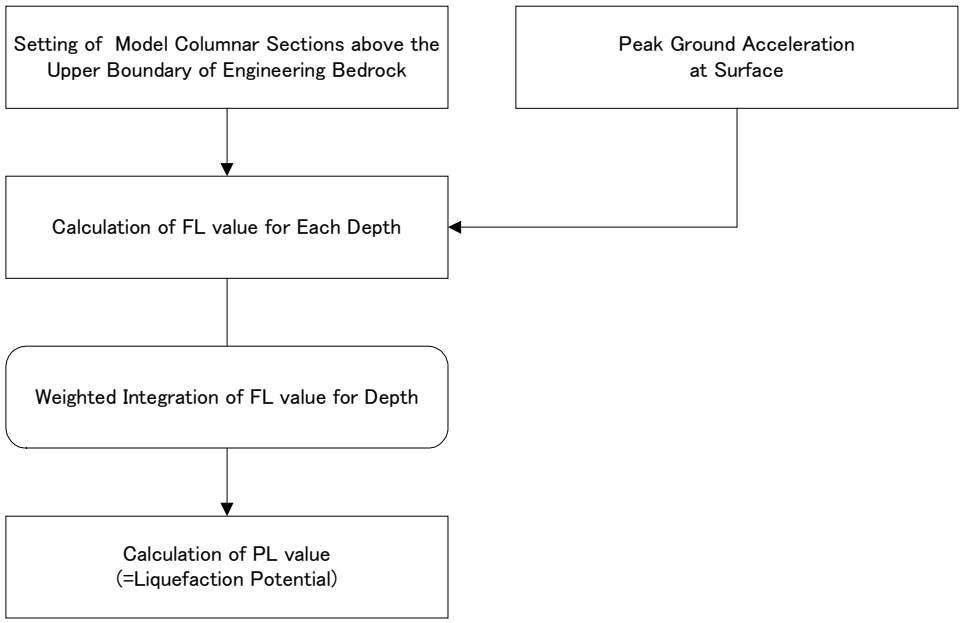

Figure 2.3.8-20 Flow chart of estimation of liquefaction potential

a) Modeling of soil

The required liquefaction parameters include the depth of layers, penetration test values, fine-grain proportion and central grain size. We used the values of actual columnar sections of wells as the depth of layers and the values acquired in the soil test in the Guatemala City area as the grain size, respectively. As to the penetration test values, we applied the experiment result in Japan shown in Figure 2.3.8-21 to the similar facies in Guatemala and estimated penetration test values (N-values) from the values of S-wave velocities.

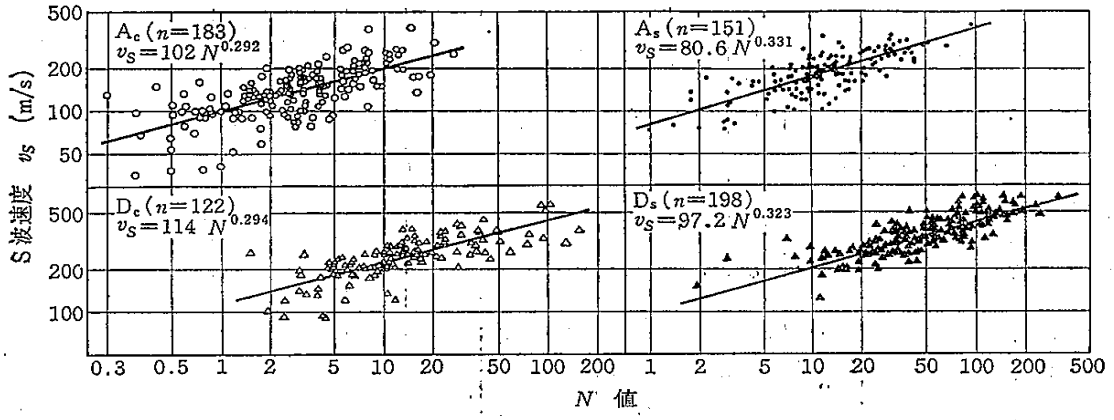

Figure 2.3.8-21 Relationship between S-Wave velocities and sounding values (N-values) by soil types (Imai, 1977)

Vertical axis: S-wave velocity, Horizontal axis: N-value, Ac: Alluvial clay, DC: Pleistocene clay, As: Alluvial sand, Ds: Pleistocene sand

Note: An N-value (penetration test value) represents the number of times in which a split spoon sampler 35 mm in internal diameter, 51 mm in external diameter, and 810 mm in length, placed on the bottom of a hole, must be hit by a hammer weighing 63.5 kg from a height of 75 cm until the sampler penetrates the soil for 30 cm.

b) Major characteristics of values

♦ N-value (Penetration test value)

The standard penetration test used to acquire an N-value, executed commonly in Japan, is an in-situ experiment that enables simple identification of soil strength. Similar test values were attached to the data of borings executed in the lowland in the Puerto Barrios area.

According to the S-wave velocities, pyroclastic flow deposits in the Guatemala City and Quetzaltenango areas are assumed with an N-value of 10 to 15 in the upper part and around 25 to 35 in the middle to lower parts, respectively. Pumice fall beds in the

uppermost part should have an N-value of 7 to 8. Among the alluvial formations found in various areas, the viscous soil has an N-value of 1 to 2 while the alluvial sand and silt in Puerto Barios have an N value of around 2 to 4. Elsewhere in the Escuintla and Mazatenango areas, there are mainly deposits mixed with conglomerates, resulting in an N-value of over 50.

♦ Fine-grain proportion

The fine-grain proportion, a total ratio of silt and viscous soil, is around 26 to 33% for pumice deposits or below 20% for pumice fall beds.

c) Groundwater level

The groundwater levels listed in the data of wells in the Guatemala City area are shallow in the valleys and deep on the plateaus. A groundwater level is 5 meters or shallower at the minimum and 150 meters or deeper at the maximum. The groundwater may permeate quickly through the facies of pyroclastic flow deposits, because of many cavities and little fine grains and thus the groundwater table may not be identified until it is fairly deep (about 50 to 70 meters). However, even if no continuous aquifer is formed, there may be a groundwater level due to perched water near the surface layer in some places. In the Quetzaltenango area, the groundwater level is deep as shown by the data of columnar sections of wells, which indicate many groundwater levels deeper than 50 meters. In the columnar sections of wells in the Mazatenango area, thick, conglomerate facies make up an aquifer but the groundwater level is deeper than 70 meters. In the Escuintla area, according to estimations, the groundwater level is shallower than 5 meters because there is an argillaceous portion above the conglomerate deposits. The groundwater level is shallower than 5 meters in the lowland area and 10 to 20 meters in the hilly terrain in the Puerto Barrios area.

Table 2.3.8-10 Ground water level in each study area

Study area	Ground type (landform)	Ground water level
Guatemala city	Pumicious sand (valley plain)	<5m
	Pumice (upland)	50m～150m
	Bedrock (hill)	—
Quetzaltenango	Pumicious sand (valley plain)	<5m
	Pumice (upland)	>50m
	Bedrock (hill and volcano)	—
Mazatenango	Gravel and ash (volcanic fan)	>70m
Escuintla	Gravel and silt (debris flow)	<5m
Puerto Barrios	Sand and silt (lowland)	<5m
	Bedrock (hill)	10m～20m

d) Outline of the method

The FL method is used to recognize the liquefaction potential at each depth, while the PL method is used to estimate the liquefaction potential of the entire soil.

♦ F_L (Factor of safety for liquefaction) method

The F_L method (Japan Road Association, 1996) allows calculating an F_L value at an arbitrary depth and recognizes the liquefaction potential at this depth. The relationship between the F_L value and the liquefaction potential is shown in Figure 2.3.8-11.

Table 2.3.8-11 Legend of F_L value

$F_L > 1.0$ -- There is little possibility of liquefaction at the depth.
$F_L <= 1.0$ -- There is the possibility of liquefaction at the depth.

♦ PL (Potential for liquefaction) method

An F_L value is used to estimate the liquefaction potential at a certain depth but not the liquefaction potential of the entire soil. Therefore, the liquefaction potential of the entire soil was estimated using a P_L value proposed by Iwasaki et al. (1980). A P_L value, obtained by weighting an F_L value for the depth up to 20 meters according to the depth and integrating it, is used to estimate the liquefaction potential of the entire soil. The relationship between a P_L value and the liquefaction potential is shown in Figure 2.3.8-12. We used a P_L value to estimate the liquefaction potential.

Table 2.3.8-12 Legend of P_L value

$P_L = 0$ -- Liquefaction potential is quite low.
$0 < P_L <= 5$ -- Liquefaction potential is low.
$5 < P_L <= 15$ -- Liquefaction potential is high.
$15 < P_L$ -- Liquefaction potential is very high.

Reference

Architectural Institute of Japan (1988) Recommendations for design of building foundations (in Japanese).

Association for the development of earthquake prediction (1998) Report of review and examples for estimation method of strong ground motion (in Japanese).

Hisada, T. and H. Ando (1976) Relation between duration of earthquake ground motion and the magnitude, *Kajima Institute of Construction Technology Report* (in Japanese).

Imai, T. (1977) P and S wave velocities of the ground in Japan, *Proc. Ninth ICSMFE*, 2, 257-260.

Iwasaki, T., F. Tatsuoka, K. Tokida, and S. Yasuda (1980) Estimation of degree of soil liquefaction during earthquakes, *Soil Mechanics and Foundation Engineering*, 28, 23-29 (in Japanese).

Knudson, C. F. and V. Perez, Guatemalan strong-motion earthquake records.

Koch, A. J. and H. McLean (1975) Pleistocene tephra and ash-flow deposits in the volcanic highlands of Guatemala, *Geol. Soc. Am. Bull.*, 86, 529-541.

Schmidt, V., A. Dahle, and H. Bungum (1997) Costa Rican spectral strong motion attenuation, *Reduction of Natural Disasters in Central America Earthquake Preparedness and Hazard Mitigation Phase II: 1996-2000, Part 2.*

Schnabel, P. B., J. Lysmer and H. B. Seed (1972) SHAKE a computer program for earthquake response analysis of horizontally layered sites, *EERC*, 72-12.

Seed, H. B. (1979) Soil liquefaction and cyclic mobility evaluation for level ground during earthquakes, *J. GED, ASCE*, Vol.105, No.GT2, 201-255.

Sugito, M., G. Goda and T. Masuda (1994) Frequency dependent equi-linearized technique for seismic response analysis of multi-layered ground, *Proceedings of JSCE*, 493, 49-58 (in Japanese with English abstract).

Wald D. J., V. Quintro, T. H. Heaton, H. Kanamori, C. W. Scrivner and C. B. Worden (1999) TriNet "ShakeMaps": Rapid generation of instrumental ground motion and intensity maps for earthquakes in southern California, *Earthquake Spectra*, 15, 537-555.

(3) Volcanic hazards

1) Outline of simulation

There are four volcanoes that were evaluated: Santiaguito, Cerro Quemado, Pacaya, and Tacaná. The overall flow of volcanic hazard evaluation process is shown in Figure 2.3.8-22.

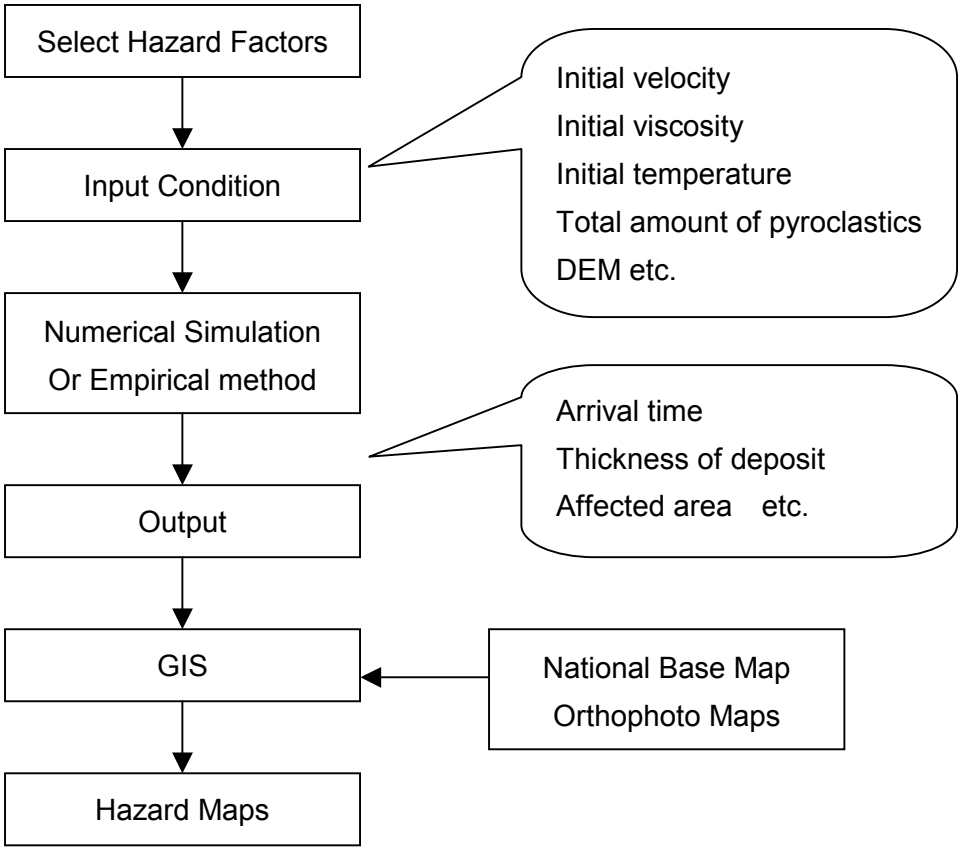

Figure 2.3.8-22 Flow chart of estimation of volcanic hazards

Following hazard types are selected to estimate for each volcano.

Table 2.3.8-13 Selection of hazard type

Volcanoes	Ash fall &Ejected Rocks	Pyroclastic flow	Lava flow	Lahar	Edifice collapse	Volcanic gas
Santiaguito	◎	◎	◎	◎	○	△
Cerro Quemado	◎	◎	◎	△	○	△
Pacaya	◎		◎	△	○	△
Tacaná	◎	○	◎	△	○	△

◎: Digital simulation ○: Simple digital simulation △: Empirical method

Evaluation method of each hazard was decided through discussion and input conditions are also decided as shown in Table 2.3.8-13.

2) Estimation of pyroclastic fall

The study team carried out numerical simulation to pursue the motion of particles of pyroclastic matter ejected into the air by using an equation of diffusion. Two types of simulation were used; for ash and ejected rocks.

a) Fall of ejected rock

① Method

The orbits of ejected rocks are analyzed during explosive eruptions of Sakurajima, Japan. The movement of rocks is described by inertial force, gravity and air drag.

$$x = V_w t \cos(\phi_w - \phi) + \frac{1}{\lambda}\log\{\lambda\, t(v\cos\theta - V_w\cos(\phi_w - \phi)) + 1\}$$

$$z = \frac{1}{\lambda}\log\sin\left(\sqrt{\lambda g}t + \cot^{-1}\sqrt{\frac{\lambda}{g}}v\sin\theta\right) + \frac{1}{\lambda}\log\sqrt{1+\frac{\lambda}{g}v^2\sin^2\theta} \quad (Ascending) \quad (t>0)$$

$$z = -\frac{1}{\lambda}\log\cosh\left(\sqrt{\lambda g}t - \tan^{-1}\sqrt{\frac{\lambda}{g}}v\sin\theta\right) + \frac{1}{\lambda}\log\sqrt{1+\frac{\lambda}{g}v^2\sin^2\theta} \quad (Descending) \quad (t>0)$$

here,

v = $V_{max}(\sin^{1.5}\theta)$,

λ = $3C_D\rho_a/4\rho_b d$,

C_D : Drag coefficient(0.2),

d : Maximum diameter of rock,

g : Gravitational acceleration,

V_{max} : Maximum initial velocity of rocks,

x : Horizontal distance from crater,

z : Height from crater,

ρ_a : Air density,

ρ_b : Density of rock,

θ : Angle of emitting direction,

ϕ : Emitting direction,

V_W : Wind velocity,

ϕ_W : Wind direction,

t : Time

② Derived results

- Arrival point

③ Necessary parameters

- Point of ejection
- Diameter and Initial velocity of ejected rocks

- Angle of emitting direction

④ Object volcano of Simulation

- Santiaguito
- Cerro Quemado
- Tacaná

b) Ash fall (pumice, scoria, volcanic ash, etc.)

① Method

The motion of particles of pyroclastic matter ejected into the air is pursued by using an equation of diffusion as shown in Figure 2.3.8-23.

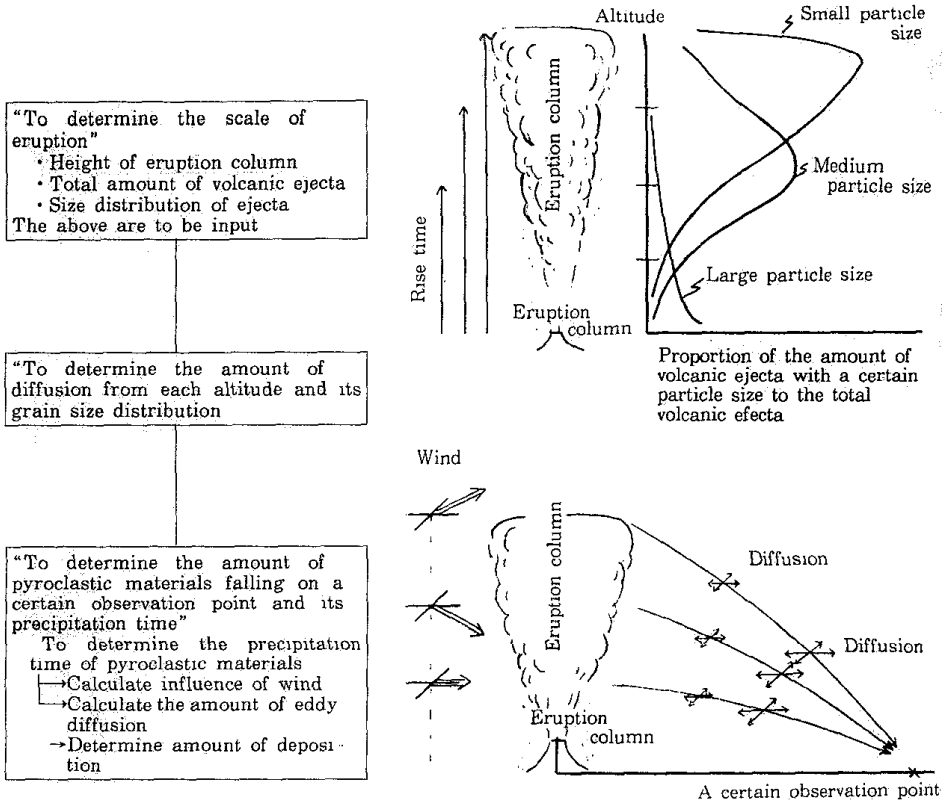

Figure 2.3.8-23 Processes in the prediction method for ash fall

② Derived results

- Thickness of ash fall
- Starting time of ash fall
- Grain size of deposit

③ Necessary parameter

- Total amount of volcanic ejecta

- Height of eruption column
- Duration of eruption
- Grain size distribution
- Wind velocity and direction

④ Object volcano of Simulation

- Pacaya
- Santiaguito
- Cerro Quemado
- Tacaná

3) Estimation of pyroclastic flow

There are two types of simulation as follows.

1. Bingham flow model to calculate motion of pyroclastic flow which occur as a result of collapse of lava
2. Energy cone model to estimate the affected area by pyroclastic flow which accompanies plinian eruption

a) Bingham flow model

① Method

Movement of pyroclastic dlow is calculated by 2-dimensional simulation using Bingham flow model, which shear stress is described as follows

$$\tau = \tau_0 + \eta \frac{du}{dz} + \frac{1}{2} C_g \rho u_m^2$$

here,

τ_0 : Yield strength,

η : Coefficient of viscosity

C_g : Drag coefficient against ground,

u_m : Mean velocity of pyroclastic flow,

ρ : Density of pyroclastic flow

② Derived results

- Affected area
- Arrival time
- Deposit thickness

③ Necessary parameter

- Total amount of pyroclastics
- Extrusion rate

④ Object volcano of Simulation

- Santiaguito
- Cerro Quemado

b) Energy cone model

① Method

Arrival distance of pyroclastic flow is calculated by use of energy line.

Energy line model treats pyroclastic flow as a point with mass. The line that connects the height of eruption column collapse and the farthest point of pyroclastic flow deposit is called as 'energy line'.

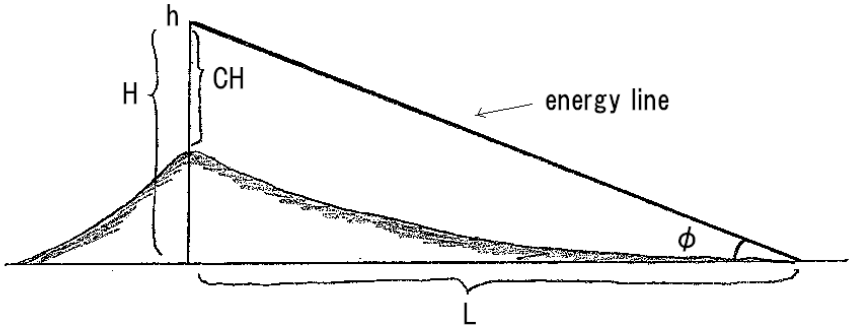

Figure 2.3.8-24 Energy Line

In Figure 2.3.8-24, $\tan\phi$ is called as 'apparent friction coefficient'. Energy cone is made from energy line by rotating around the axis of eruption column as shown in Figure 2.3.8-25.

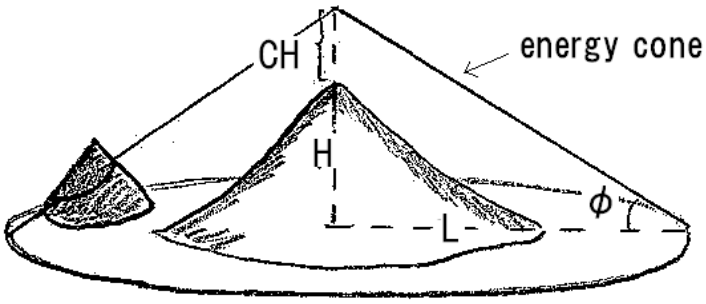

Figure 2.3.8-25 Energy Cone

② Derived results

- Farthest arrival distance of pyroclastic flow

③ Necessary parameter

- Height of eruption column collapse
- Apparent friction coefficient (H/L ratio, $\tan\phi$)

④ Object volcano of Simulation

- Santiaguito
- Cerro Quemado
- Tacaná

4) Evaluation of lava flow

① Method

Movement of lava is calculated by 2-dimensional simulation using Bingham flow model, taking cooling by radiation and mixture of lavas with different temperatures into consideration.

② Derived results

- Affected area
- Arrival time
- Deposit thickness

③ Necessary parameter

- Total amount of lava
- Extrusion rate
- Initial temperature of lava
- Initial coefficient of viscosity

④ Object volcano of Simulation

- Pacaya
- Santiaguito
- Cerro Quemado
- Tacaná

5) Evaluation of lahar

There are two types of simulation as follows.

1. 2-dimensional simulation to calculate motion of lahar
2. Empirical evaluation of affected area by lahar by use of geomorphology

a) 2-dimensional simulation

① Method

Movement of lahar is calculated by 2-dimensional simulation. Flood hydrograph is given to the upstream end of a target river to estimate the downflow of the lahar and the sedimentation process through elapse of time.

Hydrograph is derived from 'Rational formula' and flood arrival time calculated from

length and inclination of valley.

② Derived results

- Affected area
- Arrival time
- Deposit thickness
- Maximum flow depth

③ Necessary parameter

- Hydrographs
- Soil density

④ Object volcano of Simulation

- Santiaguito

b) Empirical method

① Method

Affected area by lahar is estimated by empirical method using geomorphology.

② Derived results

- Hazardous area for lahar

③ Necessary parameter

- Geomorphology

④ Object volcano of Estimation

- Pacaya
- Santiaguito
- Cerro Quemado
- Tacaná

6) Evaluation of edifice collapse

① Method

Arrival distance of debris avalanche is derived by energy line model which treats debris avalanche as a point with mass. The line that connects the slope height of the body and the farthest point of traveled debris avalanche is called as 'energy line'.

Energy cone is made from energy line by rotating as that of pyroclastic flow

② Derived results

- Farthest arrival distance of debris avalanche

③ Necessary parameter

- Section of collapse

- Apparent friction coefficient (H/L ratio, tan ϕ =1/5～1/15)

③ Object volcano of Simulation

- Pacaya
- Santiaguito
- Cerro Quemado
- Tacaná

7) Evaluation of volcanic gas

① Method

Affected area by volcanic gas is estimated by empirical method taking landform and crater location into consideration.

② Derived results

- Hazardous area for volcanic gas

③ Necessary parameter

- Landform

④ Object volcano of Simulation

- Pacaya
- Santiaguito
- Cerro Quemado
- Tacaná

Table 2.3.8-14 Simulation parameters (Tacaná, Santiaguito) (1/2)

Volcano	Disaster Factor	Parameter	Value	Unit	Reason or Example
Tacaná	fall of ejected rock	Initial velocity	150, 200,250	m/s	
		Angle of emitting direction	63	degree	
	ashfall	Total amount of volcanic ejecta	2.23E+13	kg	Same as Santa Maria
		Height of eruption column	29	km	〃
		Duration of eruption	20	hours	〃
		Constant K_m	1.60E+06	kg/km^4hour	〃
		Central grain size	0.1	cm	
		Standard deviation of grain size	1.0		
		Coefficient K_r	0.198		(Suzuki, 1990)
		Constant C	400	$cm^2/sec^{5/2}$	(Suzuki, 1990)
		λ	1 or 1/2		
		Particle shape factor (b+c)/2a	2/3		
		Mean density of falling pyroclastic materials with several cm in diameter	1.0	g/cm^3	
		Air density (Sea level)	1.226E-01	g/cm^3	
		Air viscosity coefficient (sea level)	1.80E-04	poise	
		Wind velocity vector			
		Constant β	0.069		
		Constant α	1.0-3.5E-05		
	pyroclastic flow	Height of eruption column collapse	50	m	
		H/L ratio	0.25,0.2,0.1		
	lava flow	Total amount of lava	0.045	km^3	$1.5km^2 \times 30m$
		Extrusion rate of lava	2,000	m^3/s	
		Duration of extrusion of lava	6.25	hours	from above two parameters
		Initial temprature of lava	1,000	degree	dacite
		Initial coefficient of viscosity of lava	1.00E+09	poise	dacite
		Mesh size of calculation	40	m	
	edifice collapse	H/L ratio	0.2,0.1,0.07		1/5～1/15
Santiaguito	fall of ejected rock	Initial velocity	150, 200,250	m/s	
		Angle of emitting direction	63	degree	
	ashfall	Total amount of volcanic ejecta	2.23E+13	kg	William & Self (1983)
		Height of eruption column	29	km	〃
		Duration of eruption	20	hours	〃
		Constant K_m	1.60E+06	kg/km^4hour	from above three parameters
		Central grain size	0.1	cm	
		Standard deviation of grain size	1.0		
		Coefficient K_r	0.198		(Suzuki, 1990)
		Constant C	400	$cm^2/sec^{5/2}$	(Suzuki, 1990)
		λ	1 or 1/2		
		Particle shape factor (b+c)/2a	2/3		
		Mean density of falling pyroclastic materials with several cm in diameter	1.0	g/cm^3	
		Air density (Sea level)	1.226E-01	g/cm^3	
		Air viscosity coefficient (sea level)	1.80E-04	poise	
		Wind velocity vector			
		Constant β	0.069		
		Constant α	1.0-3.5E-05		
	pyroclastic flow	Total amount of pyroclastics	0.015	km^3	1922 pyroclastic flow
		Extrusion rate	150,000	m^3/s	—
		Duration of extrusion of pyroclastics	100	sec	from above two parameters
		Density of pyroclastics	1,300	kg/m^3	
		Coefficient of viscosity	90	Pa・s	
		Yield strength	850	Pa	
		Coefficient of resistance of ground	0.01		
		Time interval of calculation	0.05	sec	
		Mesh size of calculation	40	m	
	lava flow	Total amount of lava	0.045	km^3	$1.5km^2 \times 30m$, 2000lava

Simulation parameters (Cerro Quemado, Pacaya) (2/2)

Volcano	Disaster Factor	Parameter	Value	Unit	Reason or Example
Cerro Quemado	fall of ejected rock	Initial velocity	150, 200,250	m/s	
		Angle of emitting direction	63	degree	
	ashfall	Total amount of volcanic ejecta	2.23E+13	kg	
		Height of eruption column	29	km	
		Duration of eruption	20	hours	
		Constant K_m	1.60E+06	kg/km^4hour	(Suzuki, 1990)
		Central grain size	0.1	cm	
		Standard deviation of grain size	1.0		
		Coefficient K_r	0.198		(Suzuki, 1990)
		Constant C	400	$cm^2/sec^{5/2}$	(Suzuki, 1990)
		λ	1 or 1/2		
		Particle shape factor (b+c)/2a	2/3		
		Mean density of falling pyroclastic materials with several cm in diameter	1.0	g/cm^3	
		Air density (Sea level)	1.226E-01	g/cm^3	
		Air viscosity coefficient (sea level)	1.80E-04	poise	
		Wind velocity vector			
		Constant ß	0.069		
		Constant α	1.0-3.5E-05		
	pyroclastic flow	Total amount of pyroclastics	0.012	km^3	1150BP lateral blast deposit
		Extrusion rate	100,000	m^3/s	−
		Duration of extrusion of pyroclastics	120	sec	from above two parameters
		Density of pyroclastics	1,300	kg/m^3	
		Coefficient of viscosity	90	Pa・s	
		Yield strength	850	Pa	
		Coefficient of resistance of ground	0.01		
		Time interval of calculation	0.05	sec	
		Mesh size of calculation	40	m	
	lava flow	Total amount of lava	0.2	km^3	MTU homepage
		Extrusion rate of lava	1,000	m^3/s	ten times of average rate
		Duration of extrusion of lava	55.6	hours	from above two parameters
		Initial temprature of lava	1,000	degree	Showa shinzan (dacite)
		Initial coefficient of viscosity of lava	1.00E+09	poise	Showa shinzan (dacite)
		Mesh size of calculation	40	m	
	edifice collapse	H/L ratio	0.2,0.1,0.07		1/5～1/15
Pacaya	fall of ejected rock	Initial velocity	100,150	m/s	
		Angle of emitting direction	63	degree	
	ashfall	Total amount of volcanic ejecta	5.98E+09	kg	Smithonian HP, 1998May20 eruption
		Height of eruption column	4	km	〃
		Duration of eruption	24	hours	
		Constant K_m	2.4-10E+05	kg/km^4hour	(Suzuki, 1990)
		Central grain size	0.1	cm	
		Standard deviation of grain size	1.0		
		Coefficient K_r	0.198		(Suzuki, 1990)
		Constant C	400	$cm^2/sec^{5/2}$	(Suzuki, 1990)
		λ	1 or 1/2		
		Particle shape factor (b+c)/2a	2/3		
		Mean density of falling pyroclastic materials with several cm in diameter	1.0	g/cm^3	
		Air density (Sea level)	1.226E-01	g/cm^3	
		Air viscosity coefficient (sea level)	1.80E-04	poise	
		Wind velocity vector			
		Constant ß	0.069		
		Constant α	1.0-3.5E-05		
	lava flow	Total amount of lava	0.09	km^3	
		Extrusion rate of lava	500	m^3/s	
		Duration of extrusion of lava	50.0	hours	from above two parameters
		Initial temprature of lava	1,000	degree	Sakurajima

(4) Landslide hazards

1) Outline of evaluation

There are two study areas for landslides with different study methods and scales. The Detailed Study Areas include Guatemala City, Quetzaltenango, and Antigua, where landform classification and slope classification will be made to assess the landslide hazards. The two Wide Study Areas include the North-West Region and Central Region, where the slope classification and distribution of landslides, etc. will be studied.

The flow of these evaluation processes is shown in Figure 2.3.8-26.

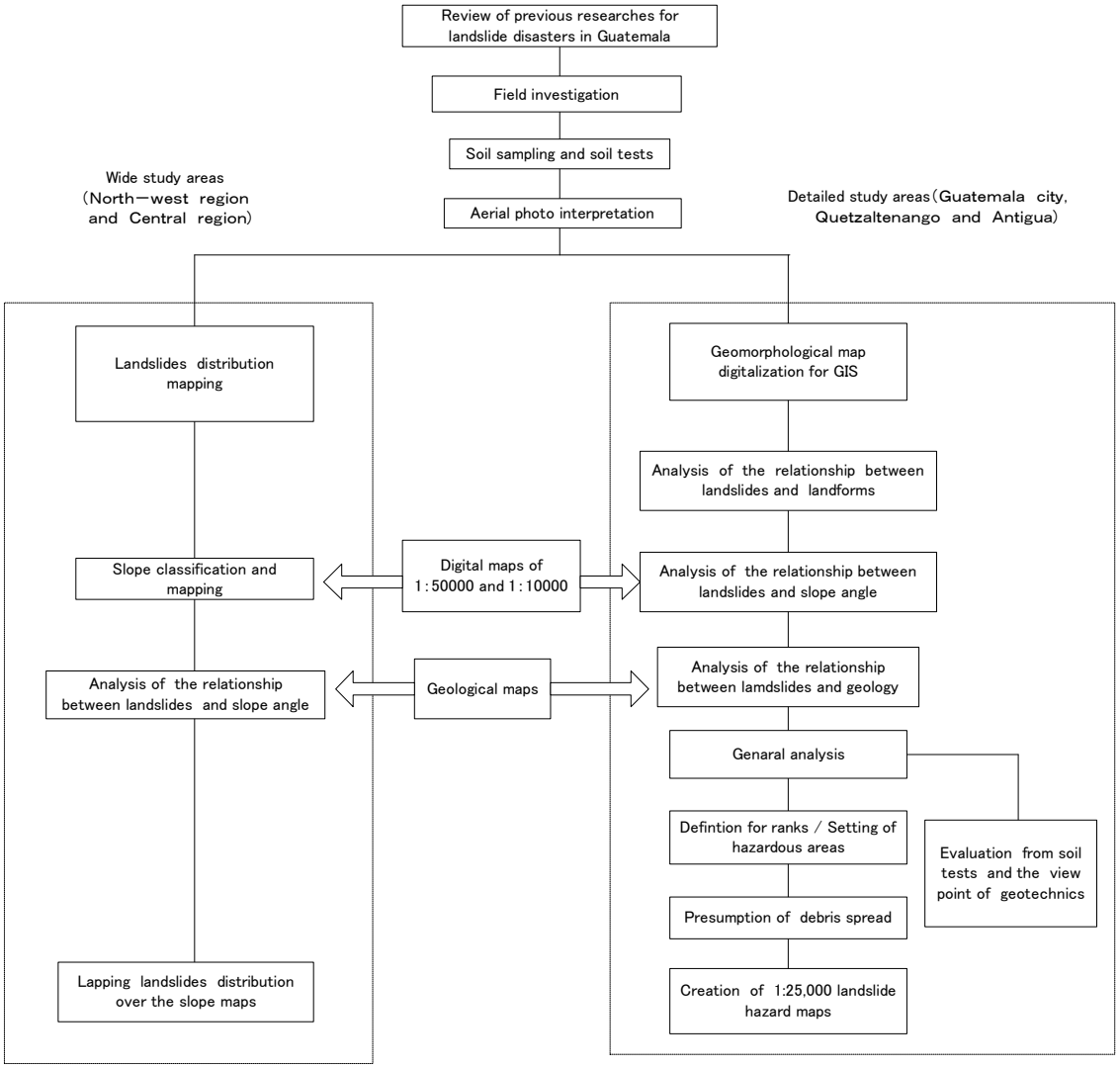

Figure 2.3.8-26 Flow of Landslide Hazard Evaluation

Note: Landslides and slope collapses are handled as different items for analysis, for the landslide evaluation.

2) Types of landslides

Landslides can be classified into so-called landslides and slope collapses. Landslides, more extensive than slope collapses, consist of those, which occur at once, and those which continue to occur intermittently for a long period of time. On the other hand, slope collapses refer to phenomena in which deeply weathered rocks and stones or unconsolidated geological strata collapse often in a selective manner. Therefore, any slope that underwent a collapse once tends to be temporarily stabilized, then become indestructible. Concerning the Los Chocoyos pyroclasitic flow deposits layer distributed near Guatemala City, any portion is likely to collapse regardless of the progress of weathering. Furthermore, the erosion of rivers is so active that the lower parts of slopes have been hollowed out to become unstable shapes in many places.

Stones and rocks are often exposed on the faces of slopes on roads, where rock falls tend to occur. Furthermore, heavy rainfall tends to cause debris flows in mountain streams and small concave slopes.

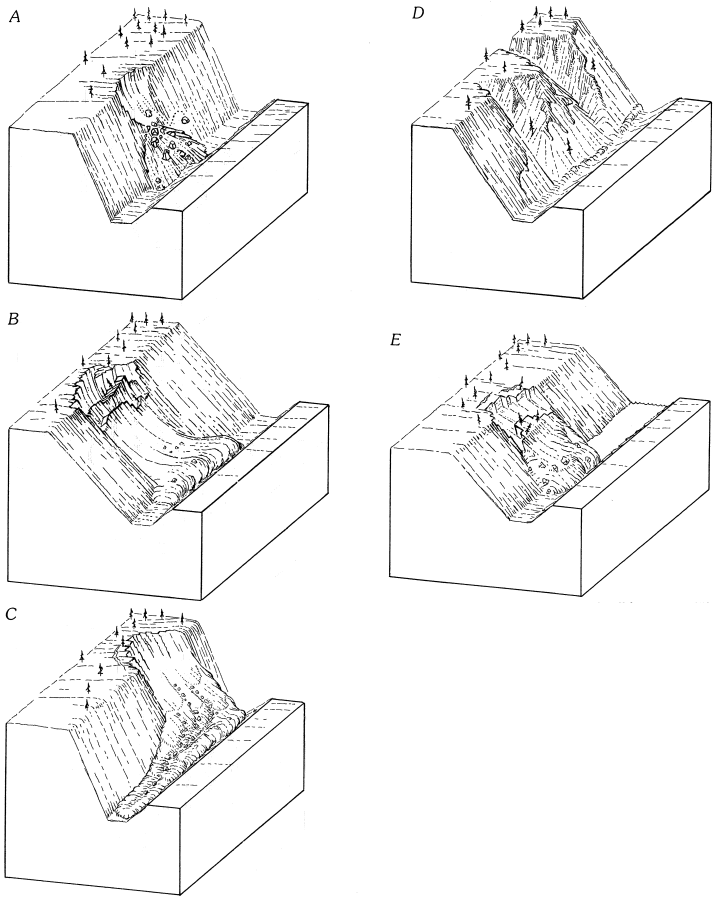

Figure 2.3.8-27 Types of landslides generated by 1976 Guatemalan earthquake
Edwin L.Harp, Gerald F. Wieczorek, and Raymond C. Wilson (1981)

3) Detailed study areas (Guatemala city, Quetzaltenango and Antigua)

a) Relationship between landslides and landforms

The maps showing distribution of landslides and slope collapses in the three areas are shown in Figure 2.3.8-28, Figure 2.3.8-29, and Figure 2.3.8-30. These maps are based on interpretation of aerial photographs, supplementary field survey, and information supplied by Mr. Manuel Mota of INSIVUMEH.

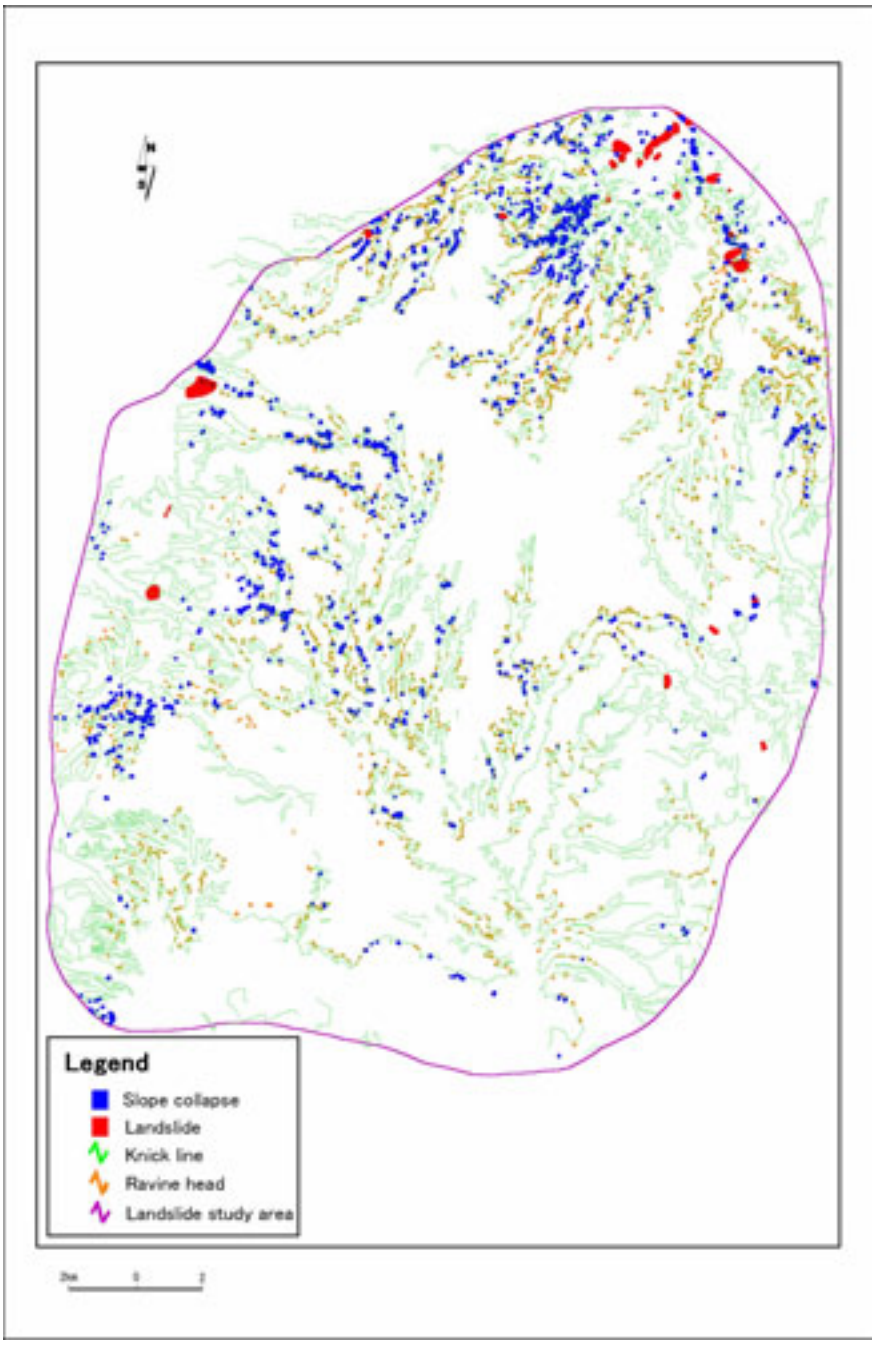

Figure 2.3.8-28 Landslide and slope collapse distribution in Guatemala City Area

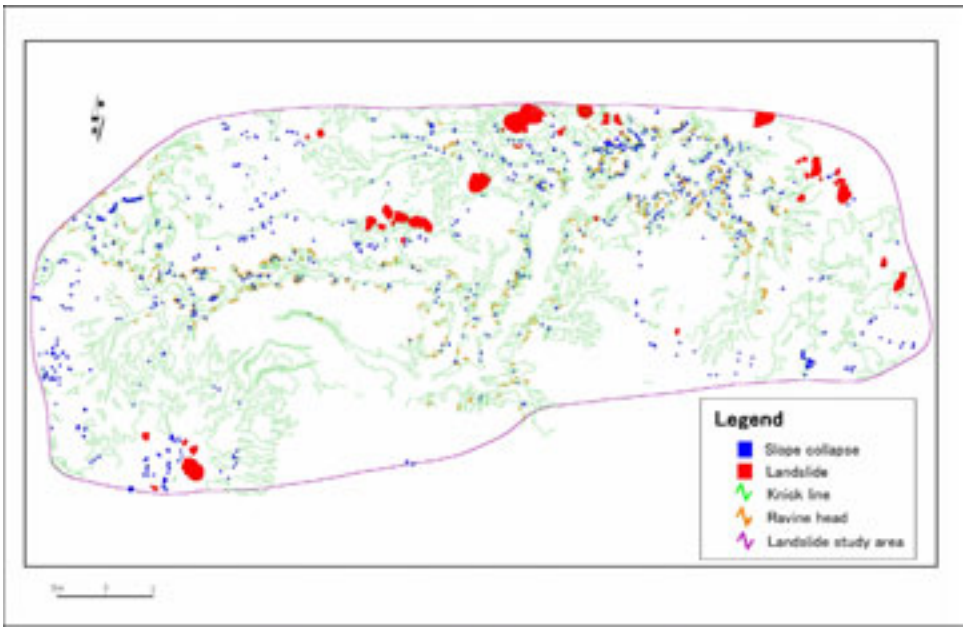

Figure 2.3.8-29 Landslide and slope collapse distribution in Quetzaltenango Area

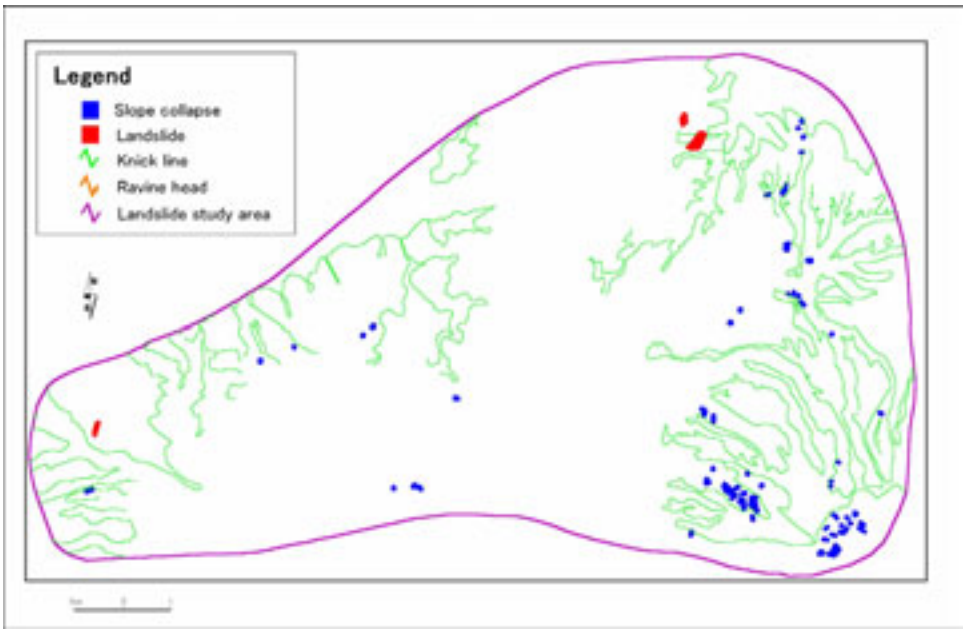

Figure 2.3.8-30 Landslide and slope collapse distribution in Antigua Area

The distribution of these landslides was superimposed over the geomorphological map acquired through interpretation of aerial photographs to understand the relationship between landslides and landforms. Many of the landslides observed around Guatemala City were caused by the earthquake that struck in 1976. In particular, the landslides and slope collapses caused at that time still remain in "Zonas" 1, 6, 7, and 19.

Through the interpretation of aerial photographs and field survey, we extracted knick lines and ravine heads. These landforms, closely related with slope collapses, are

especially remarkable from the viewpoint of historical geomorphology. Specifically, each of these landforms, a sign of a slope collapse in the past or start of hollowing of a valley, indicates that there will be a high hazard of slope collapse in the future.

b) Evaluation of slope collapse hazard

a. Relationship between slope collapse and geomorphological type

Next, the relationships between landform classifications and slope collapses were examined. Figure 2.3.8-31 shows the area ratios of geomorphological types in the three areas subject to detailed study. Slopes occupied about half the area, followed by pyroclastic flow plateaus occupying about 30% of the total area.

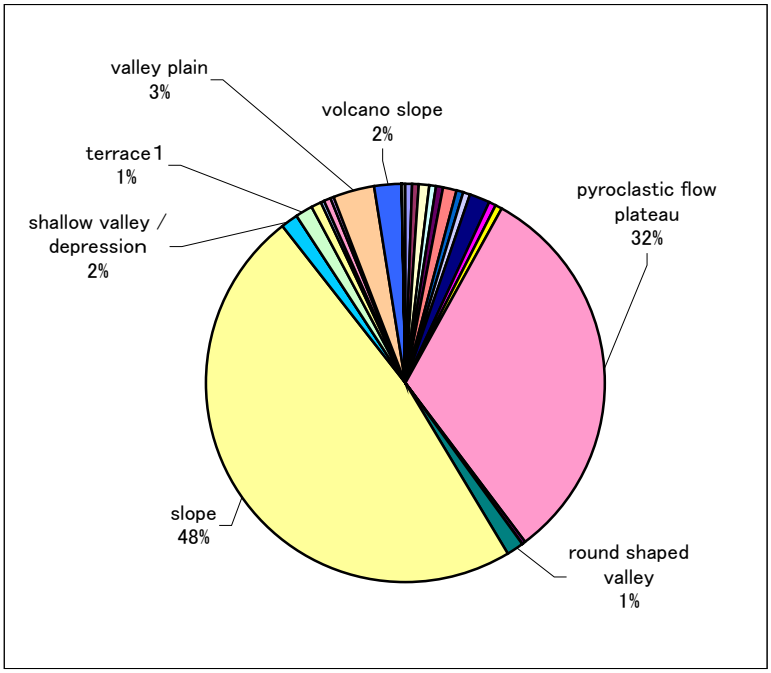

Figure 2.3.8-31 Area Ratio of Geomorphological Type in Three Areas Subject to Detailed Study

The numbers of slope collapses in the three areas by geomorphological types are shown in a graph (Figure 2.3.8-32). Naturally, slope collapses were concentrated on slopes. When observed in terms of the number of slope collapses by geomorphological types per unit area (Figure 2.3.8-33), slope collapses were concentrated on slopes all the same.

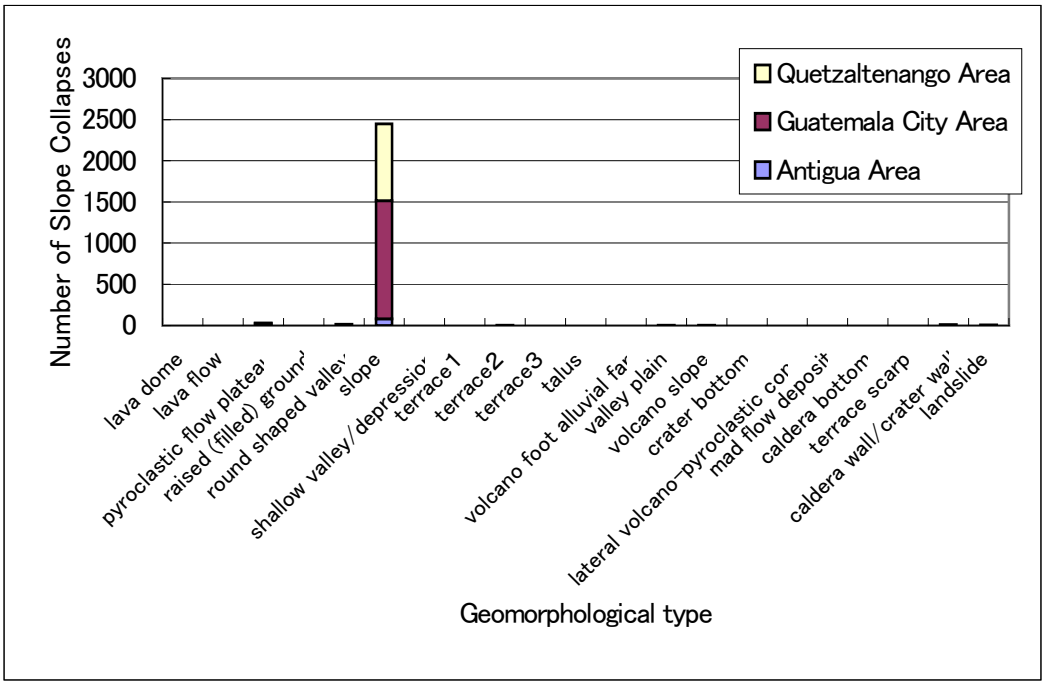

Figure 2.3.8-32 Number of slope collapses by geomorphological type (All)

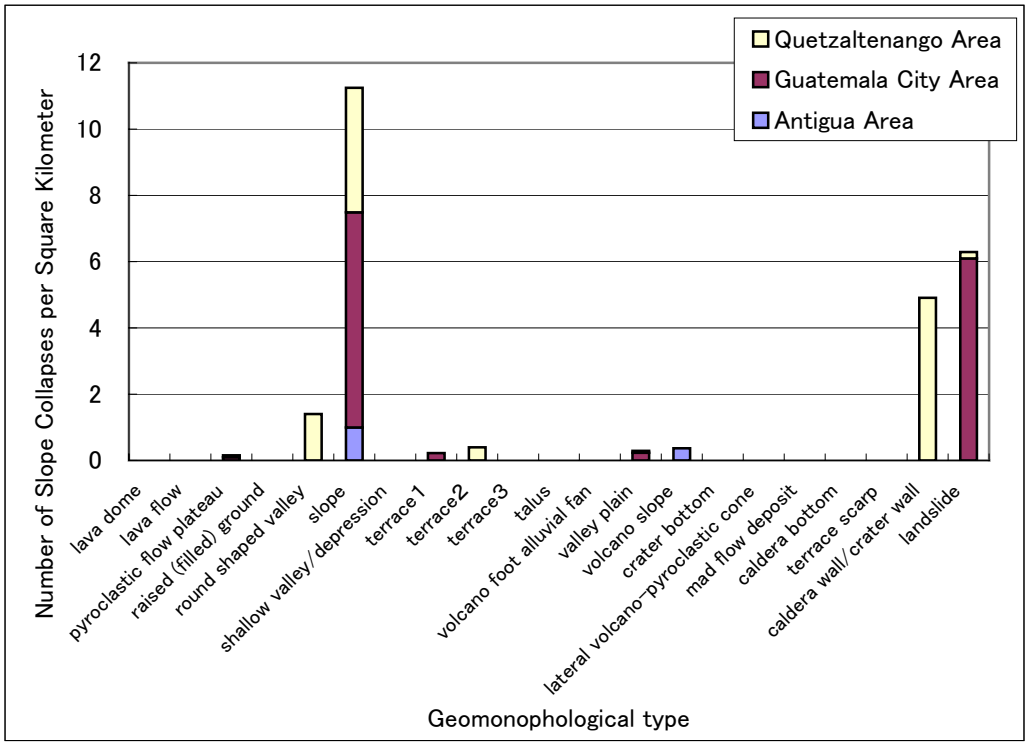

Figure 2.3.8-33 Number of slope collapses by geomorphological type (per 1 km^2)

b. Relationship between slope collapses and slope angles

The distribution of slope collapses in the three areas was superimposed over the inclination data created from digital maps with a scale of 1 to 10,000 to understand the

relationships between slope collapses and slope angles (Figure 2.3.8-28 to Figure 2.3.8-30 and Figure 2.3.8-34 to Figure 2.3.8-36).

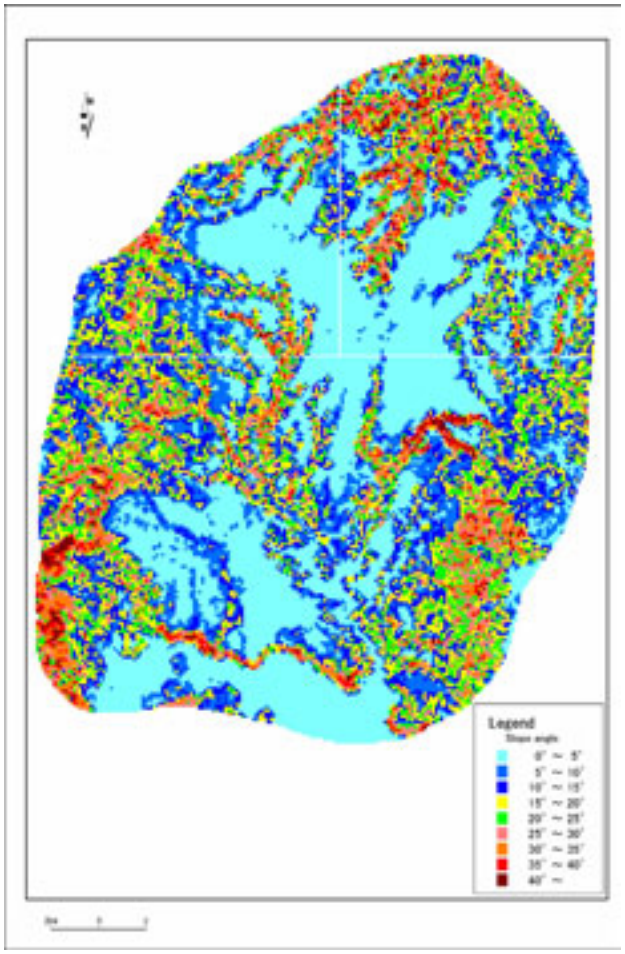

Figure 2.3.8-34 Slope angle classification map in Guatemala City Area

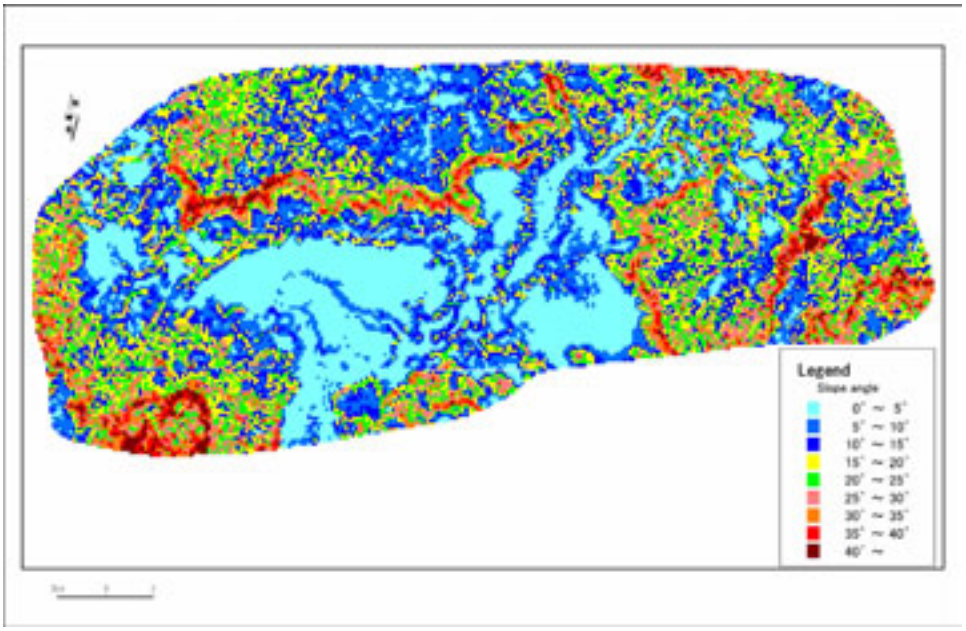

Figure 2.3.8-35 Slope angle classification map in Quetzaltenango Area

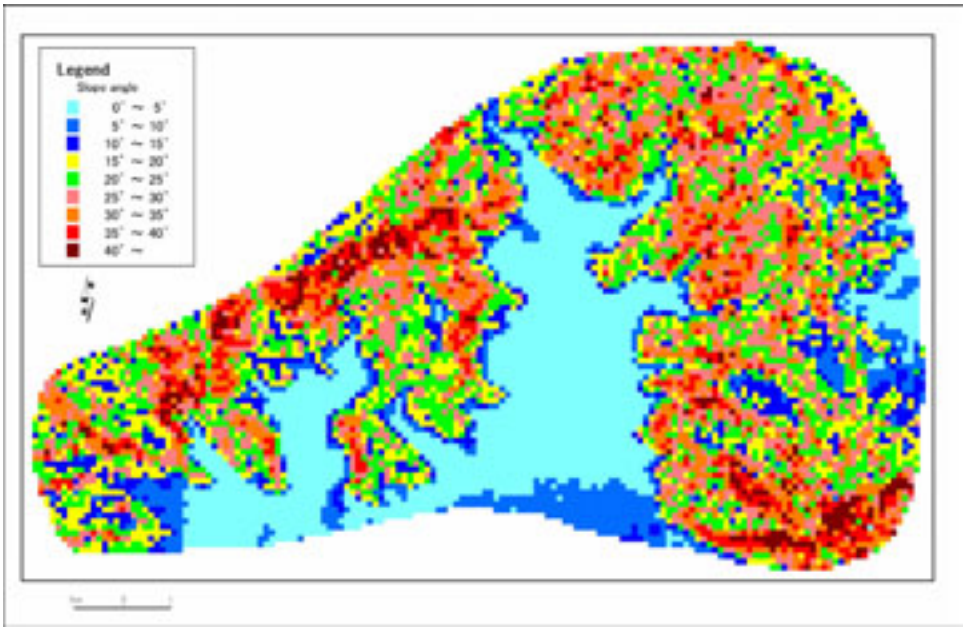

Figure 2.3.8-36 Slope angle classification map in Antigua Area

Many slope collapses occurred on slopes with angles of about 15° to 40° . When observed in terms of slope angles in steps of five degree, the number of slope collapses roughly exhibits normal distribution (Figure 2.3.8-37). There are the most slope collapses at angles of 15° to 35° , accounting for 70% of the total number of slope collapses. The second most slope collapses occur at s of 10° to 15° and 35° to 40° , accounting for 20% of the total. The number of slope collapses that occurred at angles of 0° to 10° and 40° and more accounted for only about 10% of the total.

The data on knick lines and ravine heads has problems in the way the features were counted and thus does not necessarily agree with the actual status. As far as the output image data is concerned, however, both of these features match the ravines (steep slopes) that erode a slope or pyroclastic flow and frequently overlaps with the locations of collapses. Therefore, a slope collapse or landslide is likely to occur in the future there.

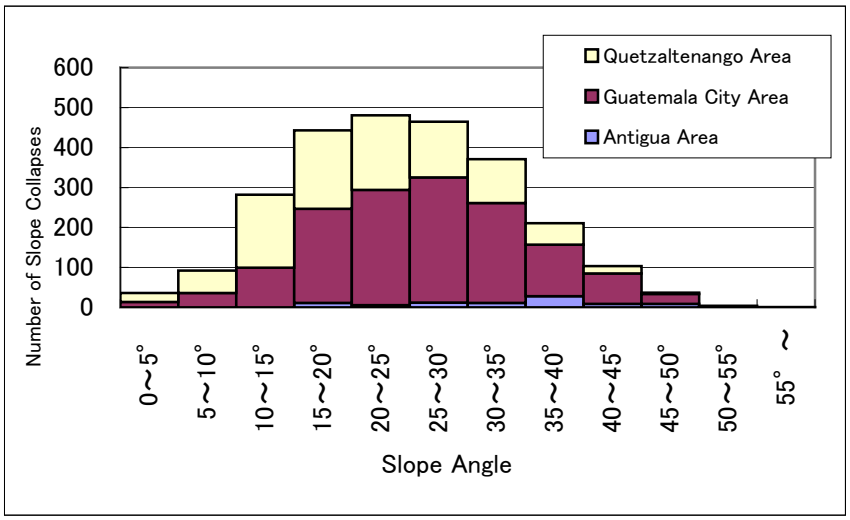

Figure 2.3.8-37 Number of Slope Collapses by Slopes (All)

Figure 2.3.8-38 shows the number of slope collapses by angles per unit area. Few slope collapses are expected to occur at angles of 0° to 10° . The steeper a slope over an angles of 10° , the more the slopes collapses. A slope collapse is the most likely to occur at angles of 40° to 50° . Especially in the Guatemala City area, the most collapses occurred at angles of 40° to 50° .

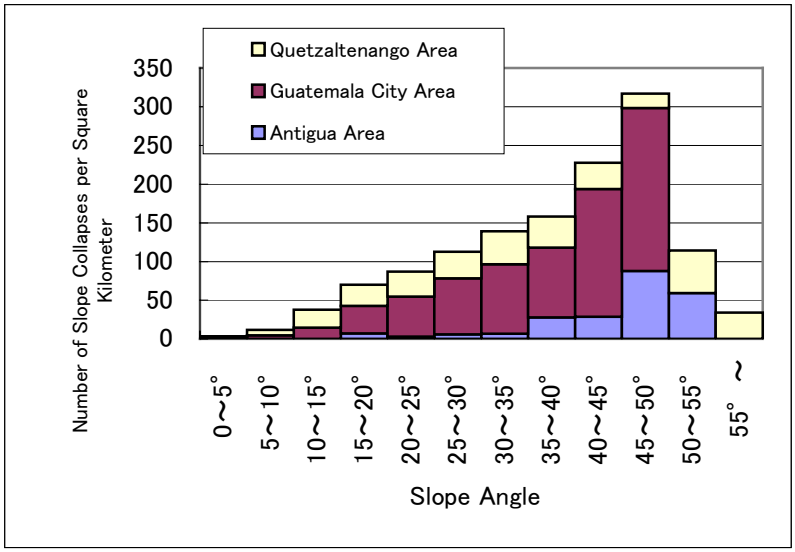

Figure 2.3.8-38 Number of slope collapses by slopes angles per Square Kilometer

c. Relationship between slope collapses and geology

The distribution of slope collapses in the three areas was superimposed over the geological data with an accuracy corresponding to a scale of 1 to 250,000 provided by MAGA to understand the relationships between slope collapses and geological features (Figure 2.3.8-39). Geological data, having a completely different investigation precision

from geomorphological map data, is very brief. For this reason, we added data for the northwestern and central areas to increase the number of samples and improve the precision in order to study the relationships between geological data and slope collapses.

The frequency of slope collapses is outstandingly high in Qp (Quaternary Pumice) and Tv (Tertiary Volcanic Rocks). The number of collapses per unit area is outstanding in Op and Tv and high also in I (Plutonic rocks), KSd (Cretaceous Sedimentary Rocks) and Qv (Quaternary Volcanic Rocks).

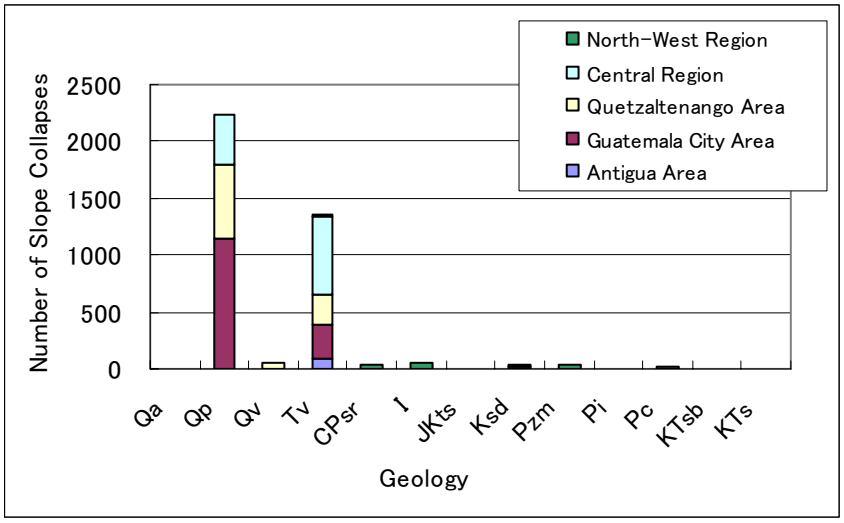

Figure 2.3.8-39 Number of slope collapses by geological features (All)

Qa:Quqternary Alluvial Deposits, Qp:Quaternary Pumice, Qv:Quaternary Volcanic Racks, Tv:Tertiary Volcanic Rocks, CPsr (Carboniferous to Permian Sedimentary, Rocks and Metamorphic Rocks), I:Plutonic rocks, JKts:Jurassic to Cretaceous Sedimentary Rocks, KSd:Cretaceous Sedimentary Rocks, Pzm:Paleozoic Metamorphic Rocks, Pi:Paleozoic Plutonic Rocks, Pc:Permian Sedimentary Rocks, Tsb:Cretaceous to Tertiary Sedimentary rocks, Kts:Cretaceous Sedimentary Rocks

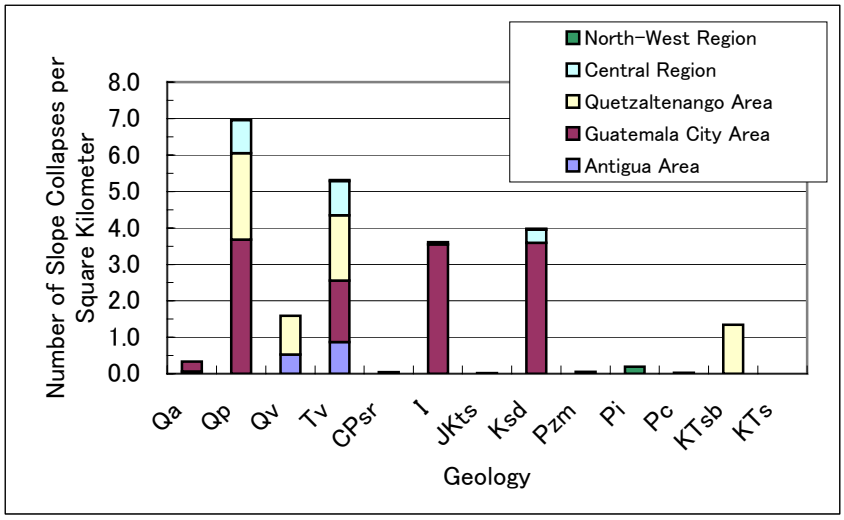

Figure 2.3.8-40 Number of slope collapses by geological features per square Kilometer

Abbreviation of geological type are same as Figure 2.3.8-39.

Regional fracture system, for example lineaments and faults in Guatemala city area are found to have an influence, though indirect in the distribution of earthquake induced landslides.

The landslides[1] caused by the Guatemala Earthquake that struck in 1976 consist, by geological features, of about 90% in the distribution area of Pleistocene pumice deposits such as Los Chocoyos pyroclasitic flow deposits, about 10% in the distribution area of Tertiary volcanic rocks, and less than 1% in the distribution area of Cretaceous limestone and Paleozoic metamorphic rocks (Edwin L.Harp, Gerald F. Wieczorek, and Raymond C. Wilson, 1978).

Also it was found that the type of landslides or slope collapses depended on geology. The pumice deposits produced mostly small shallow rock falls and debris slides, while the Tertiary volcanic rocks produced most of the large landslides, including block slides and rotational slumps, and were less susceptible to rock falls and debris slides than the pumice deposits.

c) Landslide hazard evaluation

This section comments on the evaluation of landslides. As there were a few samples of landslides, we added the data for the wide-area study regions (North-west Region and Central Region) for the purpose of evaluation.

a. Landslides and inclinations

It must be noted that there is only a limited amount of data for landslides compared to that of slope collapses and that the former is a little problematic in terms of statistical reliability. It must also be noted that it is difficult to determine only one inclination for landslides that occupy a large area.

We examined the relationships between landslides and inclinations using data for the three areas subject to detailed study. Many landslides occurred at angles of 10° to 30° and some also on easy slopes with angles of 5° to 10° .

[1] The term landslide in the Report of Harp et al (1978) included the slope collapses such as are classified in the present report.

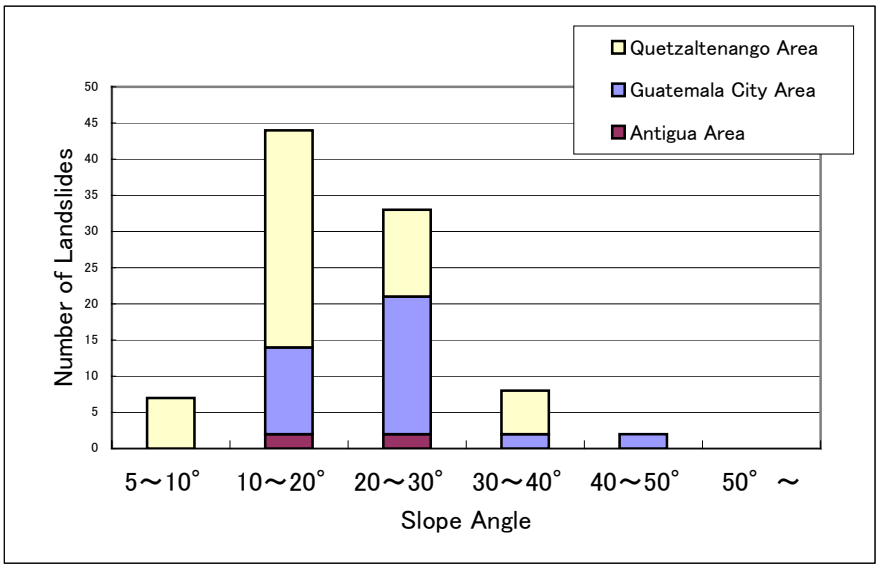

Figure 2.3.8-41 Number of locations of landslides by inclinations

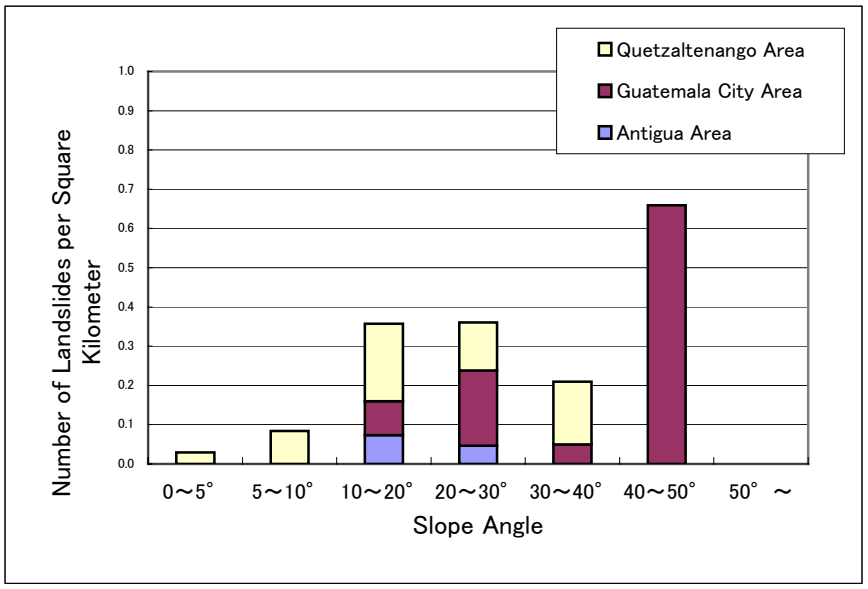

Figure 2.3.8-42 Number of landslides by slope angle per square kilometer

b. Landslides and geology

Many landslides were observed in geological features distributed in the North-west Region, i.e., CPsr (Carboniferous to Permian Sedimentary Rocks and Metamorphic Rocks), JKts (Jurassic to Cretaceous Sedimentary Rocks), I (Plutonic rocks), Ksd (Cretaceous sedimentary rocks), Pzm (Paleozoic Metamorphic Rocks) and Pc (Permian Sedimentary Rocks). In other areas, many landslides occurred in Tv (Tertiary Volcanic Rocks) and Qp (Quaternary Pumice). It can be gathered that more landslides occurred in metamorphic and sedimentary rocks.

When observed in terms of the number of landslides per unit area, landslides occurred

in Qp (Quaternary Pumice) and Tv (Tertiary Volcanic Rocks) commonly in all the areas. The outstanding result for I（Plutonic rocks）and Ksd（Cretaceous sedimentary rocks）in Guatemala City Area, and KTsb (Cretaceous to Tertiary Sedimentary Rocks) in the Quetzaltenango area drew our attention.

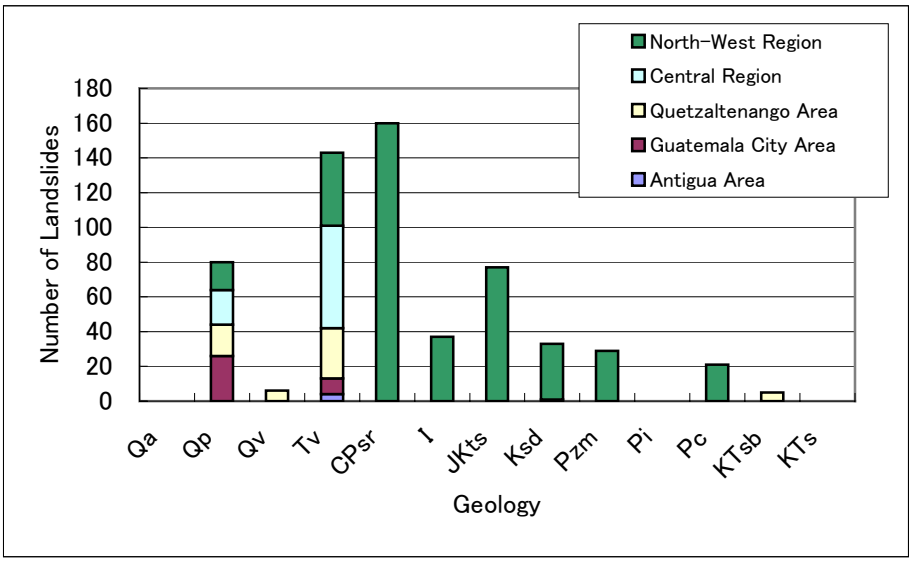

Figure 2.3.8-43 Number of Landslides by Geological Features (All)

Abbreviation of geological type are same as Figure 2.3.8-39.

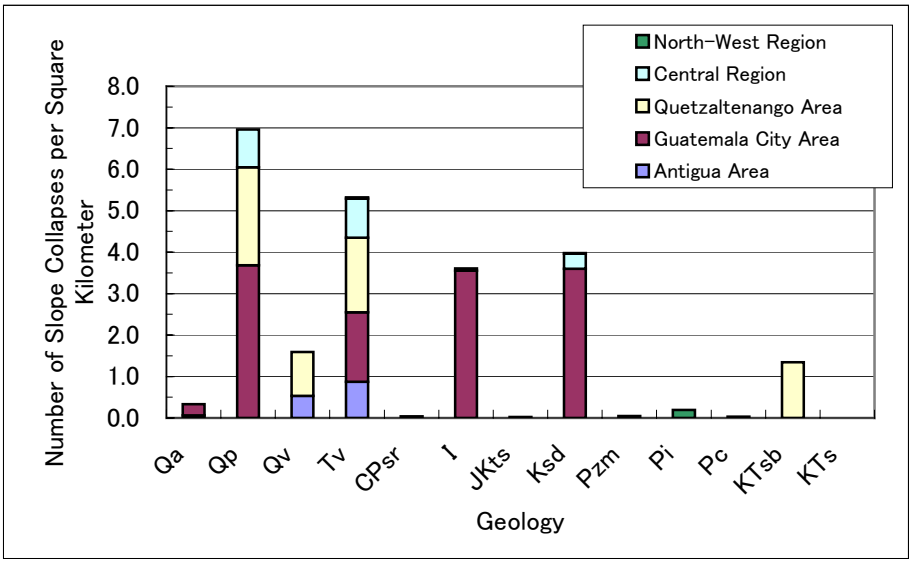

Figure 2.3.8-44 Number of Landslides by Geological Features per Square Kilometer

Abbreviation of geological type are same as Figure 2.3.8-39.

d) Provoking causes for slope collapses and landslides

It is difficult to clarify the period in which the landslides and slope collapses occurred